Talanta 107 (2013) 167–175

Contents lists available at SciVerse ScienceDirect

Talanta

journal homepage: www.elsevier.com/locate/talanta

# Rapid detection of haloarchaeal carotenoids via liquid–liquid microextraction enabled direct TLC MALDI-MS

Muthu Manikandan [a,c], Nazim Hasan [a], Hui-Fen Wu [a,b,c,d,*]

[a] Department of Chemistry, National Sun Yat-Sen University, Kaohsiung, 70, Lien-Hai Road, 80424, Taiwan
[b] School of Pharmacy, College of Pharmacy, Kaohsiung Medical University, Kaohsiung 800, Taiwan
[c] Center for Nanoscience and Nanotechnology, National Sun Yat-Sen University, Kaohsiung, 70, Lien-Hai Road, 80424, Taiwan
[d] Doctoral Degree Program in Marine Biotechnology, National Sun Yat-Sen University, Kaohsiung, 70, Lien-Hai Road, 80424, Taiwan

ARTICLE INFO

*Article history:*
Received 15 October 2012
Received in revised form
2 January 2013
Accepted 4 January 2013
Available online 12 January 2013

*Keywords:*
Haloarchaea
LLME
NPs
Carotenoid
Bacterioruberin
MALDI-MS

ABSTRACT

For the first time, we demonstrate the use of $TiO_2$ nanoparticles (NPs) for enhancing the carotenoid production by the extremophilic haloarchea, *Haloferax mediterranei*. $TiO_2$ NPs at optimal concentration of 375 mg/L results in a 95% increase in the production of carotenoid pigment compared to the control (no $TiO_2$ NPs). The carotenoid pigments extracted from $TiO_2$ NPs treated *H. mediterranei* cells, were separated using thin layer chromatography (TLC). The separated carotenoid spots were subjected directly for MALDI MS detection. To limit the sample diffusion during matrix addition on TLC plates, a simple bordering mode was exercised. Using this method we were able to detect the pigments successfully using MALDI-MS, directly from TLC plates after separation. In addition, we also applied the Pt NPs capped with ODT via Liquid–liquid microextraction (LLME) for extracting the pigment molecules from the halobacteria in MALDI-MS. These novel NP approaches possess numerous advantages such as; rapidity, ease in synthesis, high sensitivity and low cost.



## 1. Introduction

Particle size reduction to nanoscale yields materials with unique physical and chemical properties. Nanomaterials with such properties attracted researchers to exploit them in different fields such as biomedicine, optics, electronics, magnetics, mechanics, catalysis, energy science and many others [1]. In general, nanoparticles (NPs) have been synthesized using chemical methods. Controlled synthesis of nanoparticles with specific surface chemical composition and its modifications at the nanoscale is believed to fetch nanoparticles high-added value for versatile applications. Surface functionalization of nanoparticles (NPs) enables the alteration in its wetting or adhesion characteristics thereby improving its dispersion in aqueous solutions.

The application of nanomaterials is in great demand in medicine and general biology for products such as fluorescent biological labels, drug and gene delivery, bio detection of pathogens, detection of proteins and DNA, tumor destruction via heating (hyperthermia), phagokinetic studies [2]. Furthermore, nanoparticles have also proven to control human and plant pathogens of bacterial or fungal origin [3]. Although NPs have been reported in all of the above disciplines, to date, no report exists on the potential use of nanoparticles to assist/enhance the synthesis of any bio-molecules which are beneficial to human beings.

Halophilic bacteria are specialized microorganisms that inhabit hypersaline environments. These organisms express a variety of red pigments on their cell membranes which impart color to the environment in which they are found [4]. These pigments are characterized as $C_{50}$ carotenoid such as α, β γ and δ bacterioruberin [5,6]. 13 pairs of conjugated double bonds of bacterioruberin efficiently scavenge the hydroxyl free-radicals and thereby protect haloarchaea from free radical damage [7,8] and resist oxidative DNA damage resulting from radiography, UV irradiation, and $H_2O_2$ exposure [9]. Furthermore, these molecules can act as immune modulators and prophylactic agent against cancers. Therefore, they have gained paramount importance in the recent years [10]. Bacterioruberin and its derivatives have immense biological effects. Recently, an excellent review on carotenoid analysis was published by Rivera and Canela-Garayoa [11]. However, identification of these compounds from its natural source involves laborious procedures such as extraction, and identification involving the use of expensive standards.

However, the literature related to improving the production of such a valuable molecule from halobacteria is very scarce. Fang et al. [12] report a method whereby they vary the nutrients provided in the growth medium to enhance the pigment

* Corresponding author at: Department of Chemistry, National Sun Yat-Sen University, Kaohsiung, 70, Lien-Hai Road, 80424, Taiwan.
Tel.: +886 7 5252000 3955; fax: +886 7 5253908.
*E-mail address:* hwu@faculty.nsysu.edu.tw (H.-F. Wu).

0039-9140/$ - see front matter © 2013 Elsevier B.V. All rights reserved.
http://dx.doi.org/10.1016/j.talanta.2013.01.005

production. This is also a laborious process involving the standardization of each nutrient in the growth medium using a series of time consuming experiments.

MALDI-MS is a rapid and reliable technique for analysis of a wide range of biomolecules. Conventional organic matrices applied in the MALDI-MS are extremely useful for the analysis of high and low molecular weight compounds [13,14]. However, for pigment detection using the traditional matrices, the quantity of samples required to obtain a decent spectrum is extremely high. On contrary, the pigment quantity extracted by conventional extraction procedures is extremely low. Concentrating the pigments from the extracts requires either freeze drying or rotoevaporation methods which generally are time consuming and the latter perhaps may denature the compounds. NPs platforms have been used as affinity probes to selectively concentrate molecules through specific functionalization. NP based platforms for use in this direction, will be advantageous for even extremely low concentration of analytes. Liquid–Liquid Microextraction (LLME) or Single Drop Micro Extraction (SDME) in the presence of NPs was employed to selectively concentrate peptides and proteins for MALDI-MS analysis [15]. Furthermore, for MALDI MS analysis, addition of nanoparticles (NPs) to the analytes as the co-matrices or affinity probes could significantly enhance the detection sensitivity [16]. Although MALDI MS detection is rapid and easy for most biomolecule analysis, so far, NPs based capture of pigment molecules has never been reported for the concentration of carotenoid pigment molecules (bacterioruberin) to facilitate the MALDI-MS detection with extremely low amount of pigments.

In this study, for the first time, we report two novel approaches applying NPs for rapid and highly sensitive detection of pigments from halobacteria using MALDI-MS. $TiO_2$ NPs were successfully applied to induce the biosynthesis of bacterioruberin pigments from *Haloferax. mediterranei* leading to direct detection by TLC/MALDI-MS. In addition, we also employed platinum NPs for preconcentration/extraction of bacterioruberin (pigments) using octane decane thiol (ODT) functionalized Pt NPs via LLME coupled with MALDI-MS detection.

## 2. Materials and method

### 2.1. Chemicals

All the reagents used in this study are of analytical grade. 2,5-dihydroxybenzoic acid (DHB) and Trifluoroacetic acid (TFA) were purchased from Sigma Chemical Co. (St. Louis, MO, USA). Acetonitrile (MeCN) and acetone were purchased from J.T. Baker, Phillipsburg, NJ, USA. Nickel chloride ($NiCl_2$), Titanium (IV) chloride was purchased from Showa Chemicals (Japan). Chloroplatinic acid hexahydrate ($H_2PtCl_6 \cdot 6H_2O$) and 1-Octandecanthiol were bought from Alfa Aesar (Britain). Sodium borohydride ($NaBH_4$) was purchased from Koch-Light laboratories (England). Ethylene glycol, Sodium hydroxide (NaOH) and Ammonium bicarbonate were purchased from Sigma-Aldrich (St. Louis, MO, USA). The organic solvents were purchased from J.T. Baker (USA). Deionized water purified by a Milli-Q reagent system (Millipore, Milford, MA, USA) was used for all experiments.

### 2.2. Synthesis of NiO NPs

Wet chemical method was used to synthesize NiO NPs with some procedural modification described by Ai et al. [17] $NiCl_2$ (1.3 g) was dissolved in warm 1.7 mL of ethylene glycol solution. To the above solution, 0.62 g ammonium bicarbonate in 1 mL deionized water was added which resulted in green precipitation. This suspension was further stirred for 30 min at 90 °C. The precipitate was filtered off and washed with double deionized water and followed by ethanol. The green compound was dried under vacuum for 3 h at 100 °C and further calcined at 400 °C high temperature oven (Thermo scientific Model No. FB1315M, USA) for 3 h under air atmosphere. Gray black NiO obtained was further pulverized with a glass rod.

### 2.3. Synthesis of $TiO_2$ NPs

$TiO_2$ NPs were synthesized through aqueous hydrolysis of titanium (IV) chloride by precipitation with 10% NaOH solution as described by Qourzal et al. [18]. After 24 h, the deposit of hydrated titanium hydroxide was filtered off and washed with deionized water until $Cl^-$ ions are completely removed which was confirmed by silver chloride test. The solid obtained was dried at 300 °C (Thermo scientific Model No. FB1315M, USA) for 2 h. To prepare the $TiO_2$ NPs solution, a known amount of the $TiO_2$ powder was weighed accurately and re-suspended in deionized water via ultrasonication.

### 2.4. Synthesis of Pt nanoparticles modified with ODT for NP-LLME approach

The synthesis and surface modification of the Pt nanoparticles was carried out by following the method reported by Chen and Kimura [19]. Cold aqueous solution of $H_2PtCl_6$ (3.38 mM, 20 mL) was reduced by the drop wise addition of $NaBH_4$ (0.1 M, 4 mL) solution at 4 °C. The Pt nanoparticles were obtained as a black suspension when the reaction was brought to room temperature. The transparent solution of octanedecanthiol (ODT, 1.3 mmol) was prepared in 20 mL toluene, in a 100-mL Erlenmeyer flask. The above prepared Pt nanoparticle suspension was added to octandecanthiol toluene solution; two separated deferent layers appeared (lower layer was Pt NPs aqueous layer and upper organic layer of ODT toluene solution). Mixture was stirred for approximately 1 h, and finally upper layer turned deep brown which was indication for the successful Pt NPs capping with the thiol (–SH) group. FTIR analysis was used to demonstrate the shift of Pt NPs from aqueous to organic layer confirming the Pt NPs functionalization with ODT. The nanoparticles were characterized using High Resolution Transmission Electron Microscope (TEM) (JEOL TEM-3010, Tokyo, Japan) at 75 keV.

### 2.5. Microorganisms and culture media

Cryopreserved culture of *H. mediterranei* ATCC33500 was purchased from BCRC, Hsin-Chu, Taiwan. The cultures were regenerated on VKMM agar plates. The VKMM medium was prepared by dissolving 13 g of Difco nutrient broth (Bekton and Dikison Inc., USA, India), 6.35 g of KCl, 9.70 g of $MgSO_4$, 13.38 g of gelatin and 12.00 g of soluble starch in 1 L of artificial sea water prepared according to Manikandan et al. [20]. After regeneration, a single colony from the plate was inoculated into liquid broth to make a mother culture for the enhanced production of bacterioruberin by NPs treatment. NiO and $TiO_2$ were added into the VKMM medium at concentrations 125, 250, 375 and 500 mg/L. 20 mL batch of each treatment was inoculated with 0.2 mL mother culture obtained from $A_{600}$-0.6 OD in 125 ml conical flask and allowed to grow for 90 h at 42 °C under continuous light in thermostatic orbital shaker (Firstek, Taiwan) at 120 rpm speed.

### 2.6. Extraction and quantifications of pigments

After 90 h of growth, the cells of each treatment were brought $A_{600}$-15.0 in order to find the variation in pigment production at constant cell numbers. 1 mL cells from each nanoparticle

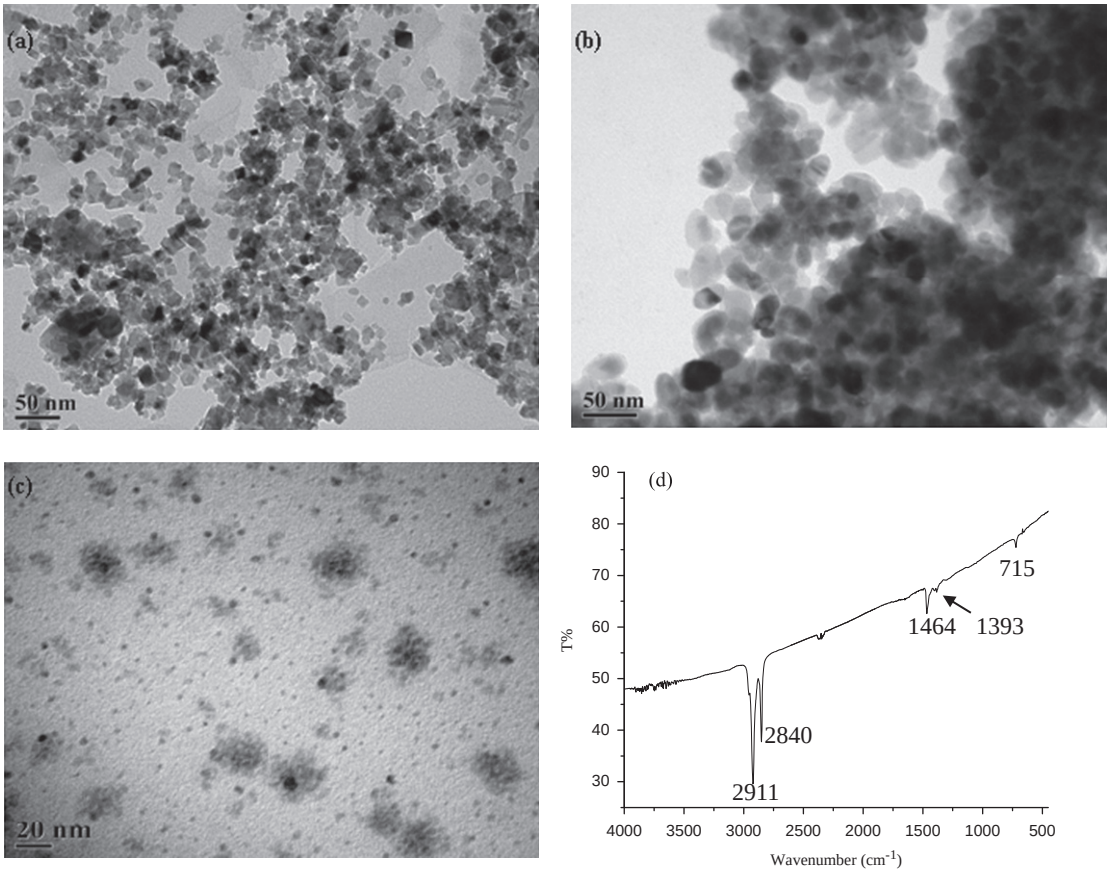


**Fig. 1.** TEM micrograph of NPs synthesized inhouse for the production enhancement and LLME for MALDI-MS detection of carotenoid pigment from *H. mediterranei*. (a) NiO NPs; (b) $TiO_2$ NPs; (c) Pt NPs; (d) FTIR spectrum confirming the ODT functionalization on the Pt NPs.

treatment were harvested by centrifugation at 10000 × g rpm for 15 min. Then, cells were suspended in acetone and stirred to extract the pigments for 10 min. The supernatant was collected from the suspension by centrifugation at 10000 × g rpm for 5 min. The pigment was extracted repeatedly as described above for three times during which the precipitate appeared hoar color. The extracts from each treatment was equalized using acetone and the absorption spectrum was obtained from 350–600 nm in a Lambda 950, spectrophotometer (Perkinelmer Inc., USA). The total carotenoid pigments quantified from each extract were determined using standard calculation for carotenoid pigments involving an average extinction coefficient [21].

### 2.7. Direct TLC/MALDI-MS detection of carotenoid pigments

The carotenoid pigments extracted from *H. mediterranei* cells treated with $TiO_2$ NPs were separated by thin layer chromatography (TLC) plates pre-coated with silica gel (Merck 5553, EMerk Inc., Germany) using 50% acetone in *n*-heptane (v/v) as a developing solvent [12]. After separation, the TLC plates were allowed to dry and the pigment spots appeared (red and orange) were marked carefully. For the TLC/MALDI-MS analysis, the silica gel particles were scraped around the spots to avoid the diffusion and spreading of pigment molecules by capillary action upon addition of matrix solution. 10 μL CHCA matrix solution (0.05 M CHCA in 3:1 Acetonitrile:Water containing 0.1% TFA) was overlaid on each spot and allowed to dry before MALDI-MS analysis. The TLC pieces containing separated spots were mounted onto a MALDI target plate with double-sided conductive adhesive tapes.

### 2.8. Platinum nanoparticle based liquid–liquid microextraction (NP-LLME) coupled with MALDI-MS for direct pigment detection from the halobacteria

10 μL (5 μg) of the crude carotenoid pigment extract from *H. mediterranei* cells was diluted to 1 mL with deionized water. 100 μL of toluene containing different concentrations (20, 40, 60, 80 and 100 μg) of platinum nanoparticles functionalized with ODT (Pt-ODT NPs) was overlaid on each diluted pigment extract and the solutions were vortexed for 5 min. Pt-ODT NPs from the toluene layer were collected by centrifugation at 15000 × g for 5 min and an equal quantity was loaded to MALDI (stainless steel) target plates, allowed to dry and 5 μL CHCA matrix (0.05 M CHCA in 3:1 Acetonitrile:Water containing 0.1% TFA) was added and analyzed.

### 2.9. MALDI-TOF MS detection

MALDI mass spectra were obtained in the positive ion mode using a MALDI-TOF MS (Microflex, Bruker Daltonics, Bremen, Germany). The MALDI source was equipped with a nitrogen laser (337 nm), a 1.25 m flight tube and the sample target having the capacity to load 96 samples simultaneously. All mass spectra were acquired with the following parameters set on the MALDI-MS: IS1, 19.0 kV; IS2, 16.15 kV; lens, 9.35 kV and reflector at 20.0 kV. The laser energy was adjusted to slightly above the threshold to obtain good resolution and signal-to-noise ratios at 60 Hz. Mass spectra from 200 Da to 2000 Da were collected in the positive ion and reflectron mode with 200 laser shots accumulated for each spectrum. For the spectral reproducibility, multiple spectrum was obtained from the target plate and reproducibility

of peaks at statistical significance was evaluated using ClinPro tools (2.1) software.

## 3. Results and discussion

### 3.1. Characterization of NiO, $TiO_2$ and Pt-ODT NPs by TEM and FT-IR

Although NPs have immense applications in a variety of fields, to date, to our best knowledge, they have not been used to enhance the production of biological molecules of commercial interests or sensitive detection for the halobacteria in the MALDI-MS. Three NPs including NiO, $TiO_2$ and Pt were synthesized inhouse and were analyzed for their size and morphology using TEM. The unmodified bare oxide NPs such as NiO and $TiO_2$ were employed for inducing the pigment biosynthesis in Haloarchaea, since these are bare NPs it is not required that we conduct FTIR (Fig. 1). The TEM micrograph of NiO NPs is shown in Fig. 1(a). The particle sizes of the indigenously synthesized NiO NPs existed in the regime of 7.5–30 nm, in which the particle with 16 and 17 nm predominated followed by the particles around 12 nm size (Fig. S1(a)). TEM of $TiO_2$ NPs are illustrated in Fig. 1(b). The size distribution of $TiO_2$ NPs were also found to be between 7.5 and 30 nm with the predomination of 12 nm particles (Fig. S1(b)). The Pt-ODT NP images are illustrated in Fig. 1(c). The synthesis of PT-ODT NPs yielded particles sized between 2 and 10 nm, among which the particle with 4 nm was predominated (Fig. S1(c)). The Pt NPS were surface functionalized with ODT for selective capture of the carotenoid pigment. The surface modification of Pt NPs with ODT was confirmed by the FTIR as shown in Fig. 1d. The C–H asymmetric and symmetric stretching frequencies of $CH_2$– groups were confirmed by absorption bands at 2911 and 2840 $cm^{-1}$. Also, the bending frequencies of C–H were observed at 1464 and 1393 $cm^{-1}$ in asymmetric and symmetric modes. This confirmed the presence of alkyl chains from ODT molecules. The absence of the thiol vibrational stretching frequency band (due to the –SH group) in the region 2600 − 2550 $cm^{-1}$ and the presence of $CH_2$–S– thiol stretching frequency at 715 $cm^{-1}$ conforms the formation of a chemical bond on Pt-ODT NPs.

### 3.2. Effect of NiO and $TiO_2$ nanoparticles on the growth and carotenoid production of the halobacteria

Initially, the *H. mediterranei* was grown in VKMM medium to analyze the growth pattern of the halobacteria (Fig. 2). The growth curve was established by assessing the growth at every 12 h for 90 h during which the organism entered into the stationary phase (Fig. 2(a)). The growth rate was measured to be 0.0683 (Fig. 2(b)) which was almost similar to the growth rate calculated for *Haloferax* sp in VKMM medium [20]. The overall optimization scheme for carotenoid production using oxide nanoparticles is given in Fig. S2. The halobacteria was treated with oxide nanoparticles such as NiO and $TiO_2$ at the concentrations range of 125–500 mg/L and 125–625 mg/L, respectively for optimizing carotenoid production. The cell concentrations in each treatment were spectrophotometrically measured at 600 nm as a difference in turbidity against uninoculated treatments. It was found that the nanoparticle treatment showed the least effect on the growth of *H. mediterranei* cells. A marginal difference on growth was observed ($16.7 \pm 0.42$–$15.5 \pm 0.54$ OD) in the NPs treated cells when compared to the untreated control ($16.9 \pm 0.22$ OD) (Fig. 2(c)). Of the NP treatments, the organism produced maximum pigment ($1.65 \pm 0.03$ mg/mL) at 375 mg/L $TiO_2$, (Table 1) followed by 500 mg/L treatment which resulted in $1.46 \pm 0.04$ mg/mL of carotenoid pigments (Fig. 3A and Table 1).

The pigment production in the other treatments such as 125, 250 and 625 mg/L treatment yielded $0.97 \pm 0.041$, $0.96 \pm 0.021$ and $0.97 \pm 0.015$ mg/mL respectively which was slightly higher than the untreated control ($0.85 \pm 0.02$ mg/mL) (Fig. 3A and Table 1).

In the case of NiO treatment on *H. mediterranei*, only marginal increase in pigment production was observed. At lowest NiO treatment (125 mg/mL), a slight improvement in pigment production was observed ($0.94 \pm 0.035$ mg/mL). With subsequent increase in the NiO NPs concentration in the growth medium, a decreased trend in pigment production was recorded as follows: $0.92 \pm 0.031$, $0.89 \pm 0.036$ and $0.57 \pm 0.015$ mg/mL for 250, 375 and 500 mg/L NiO NPs concentrations, respectively (Fig. 3B and Table 1).

The highest pigment production was calculated to be 95.4% than the control in the case of 375 mg/L $TiO_2$, followed by 72% with 500 mg/L $TiO_2$ NPs treatment. The least quantity of pigment production, 32% was observed at higher concentrations of 500 mg/L where NiO NPs showed inhibitory effects on pigment production. With the other treatments of $TiO_2$ and NiO NPs concentrations, marginal percentile increase of pigment production ranging from 4.9 to 3.8 (Table 1) was observed.

NiO NPs can induce oxidative stress to *in vitro* and also *in vivo* systems [22]. $TiO_2$ nanoparticles are also well reported to induce oxidative stress and generate oxidative free radicals such as $HO_2^{\bullet}$, $O_2^{\bullet}$, $HO^{\bullet}$ while reacting with oxygen or water [22]. However, it is also known that of the two NPs, $TiO_2$ NPs are capable of rigorous production of free radicals; this principle is that which makes $TiO_2$ efficient photocatalysts. Thus, it is understandable that compared to NiO NPs, the $TiO_2$ NPs induce more pigment production at a threshold level. Generally carotenoids are categorized as potential natural free radical scavengers. Especially, the carotenoid pigment, bacterioruberin, is considered to possess extraordinary potential to combat oxidative stress. These bacterioruberins occurring in halobacteria are the natural defense system plying to protect the bacteria from strong sunlight and subsequent free radical damage [9]. These authors report that the mode of operation depends on the highly conjugated double bonds of bacterioruberin. Therefore, these studies for the first time report that $TiO_2$ NPs at appropriate threshold concentration can act as highly potent inducers of bacterioruberin production. Fig. 4 displays the schematic of enhanced pigment production in *H. mediterranei* through free radicals generated upon $TiO_2$ nanoparticle treatment.

### 3.3. Direct MALDI-MS detection of carotenoid pigments on TLC plates

The crude pigment extract obtained from *H. mediterranei* was separated by method described by Fang et al. [12]. Four distinct pigment spots ranging from red to orange shades were obtained (Fig. 5A(a)), among which spot 1 appeared dark red compared to the rest. We measured the Rf values for each spots after TLC. The spots with Rf values of 0.62, 0.47, 0.53 and 0.28 were named as spot 1, spot 2, spot 3 and spot 4 respectively (Fig. 5A(a)). Separated pigment spots were overlaid with CHCA matrix individually and directly subjected to MALDI-MS analysis (Fig. 5A(b)–(c)). Fig. 5B(a) shows the MALDI-MS spectrum for the crude sample before separation and the direct MALDI MS detection of 4 spots obtained after separation on TLC (Fig. 5B(b)–(e)). MALDI-MS analysis of the crude sample exhibited a single carotenoid peak with a very less intensity and also the presence of other compounds with various $m/z$ values (Fig. 5B(a)). The compound in the spot 1 exhibited the $m/z$ value of about 708. 887 which was very close to previously identified bisanhydrobacterioruberin (Fig. 5B(b)). Spot 2 showed a high intensity peak at 725.315 $m/z$

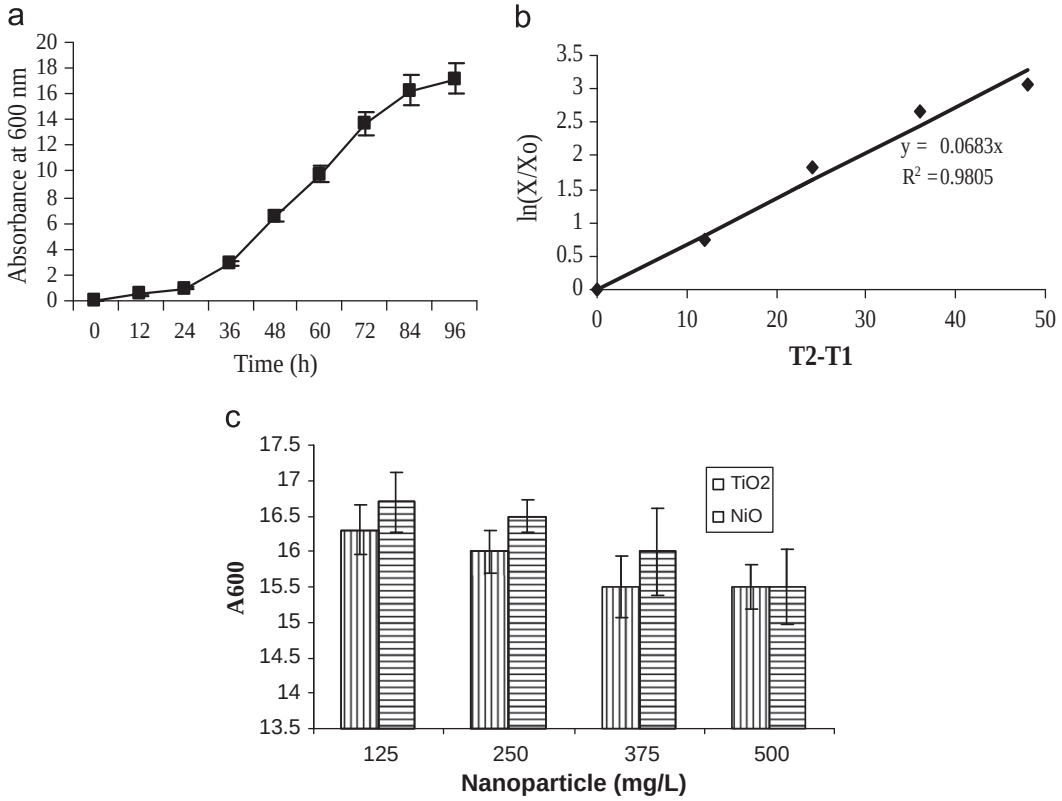


**Fig. 2.** Growth of *H. mediterranei* in VKMM medium. (a) Growth curve of *H. mediterrani*; (b) Growth rate ($\mu$) of *H. mediterranei*; (Growth rate was calculated using the equation $\ln X = \ln X_0 + \mu(t - t_0)$, where $X_0$ is the cell concentration (g $L^{-1}$) at the beginning of exponential growth phase, $t_0$ (h); and $X$ is the cell concentration (g $L^{-1}$) after a time interval $t$ (h). The intrinsic rate of growth of the microorganism under the conditions used was expressed as the specific growth rate in exponential growth phase, $\mu$, and was calculated as the slope of the plot between ($\ln X/X_0$) *versus* ($t - t_0$). (c) Optical density at 600 nm representing growth of bacteria when incubated with various concentration of $TiO_2$ and NiO NPs respectively.

**Table 1**
Influence of $TiO_2$ and NiO NPs on the carotenoid pigment production of *H. mediterranei*.

| NPs treatment | Pigment content (mg/mL from cells)[ab] | % increase/decrease of carotenoid production |
|---|---|---|
| Control | 0.85 ± 0.02 | 0 |
| $TiO_2$ 125 mg/L | 0.97 ± 0.041 | 12.01 |
| $TiO_2$ 250 mg/L | 0.96 ± 0.021 | 13.80 |
| $TiO_2$ 375 mg/L | 1.65 ± 0.03 | 95.42 |
| $TiO_2$ 500mg/L | 1.46 ± 0.04 | 72.05 |
| $TiO_2$ 625 mg/L | 0.97 ± 0.015 | 14.72 |
| NiO 125 mg/L | 0.94 ± 0.035 | 10.73 |
| NiO 250 mg/L | 0.92 ± 0.031 | 8.72 |
| NiO 375 mg/L | 0.89 ± 0.036 | 4.95 |
| NiO 500 mg/L | 0.57 ± 0.015 | −32.74 |

[a] Pigment content was calculated from extract using the OD values obtained at 494 nm and an average extinction coefficient obtained for carotenoid pigments (Liaaen-Jensen and Jensen, 1971 [21]).

[b] The Pigment content was quantified from extracts obtained from three independent experiments; the values after ± represesnt the standard experimental error.

along with some other peaks which was identified as Monoanhydrobacterioruberin based on the reference *m/z* value 724.128 (Fig. 5B(c)). Spot 3 of the TLC separation revealed the existence of a peak at *m/z* 621.608 which was believed to be a pigment peak belonging to 2-isopentenyl-3,4-dehydrorhodopin (Fig. 5B(d)) and the reproducibility of the peak (*m/z* 621.608) during the MALDI MS analysis is shown in Fig. S3; the theoretical mass value of this compound is 620.98. Finally the spot 4 of the TLC showed a very strong intensity peak at *m/z* 740.68 on MALDI-MS analysis. The *m/z* of the above peak is highly correlated with the

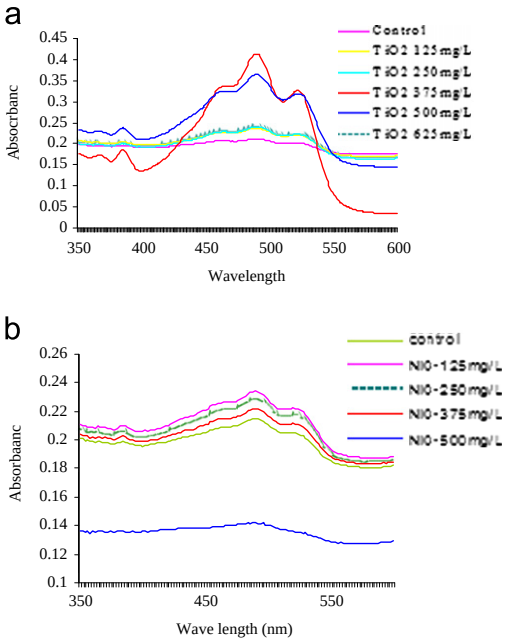


**Fig. 3.** (A) UV visible spectrum indicating pigment production of *H. mediterranei* in the presence of various concentration of $TiO_2$ NPs. (B) UV visible spectrum indicating pigment production of *H. mediterranei* in the presence of various concentration of NiO NPs. (For interpretation of the colors in this figure, the reader is referred to the web version of this article.)

bacterioruberin peak which was about 740.70 (Fig. 5B(e)). Together with the Rf and *m/z* values, all the pigment spots separated were confirmed to be carotenoid pigments using the

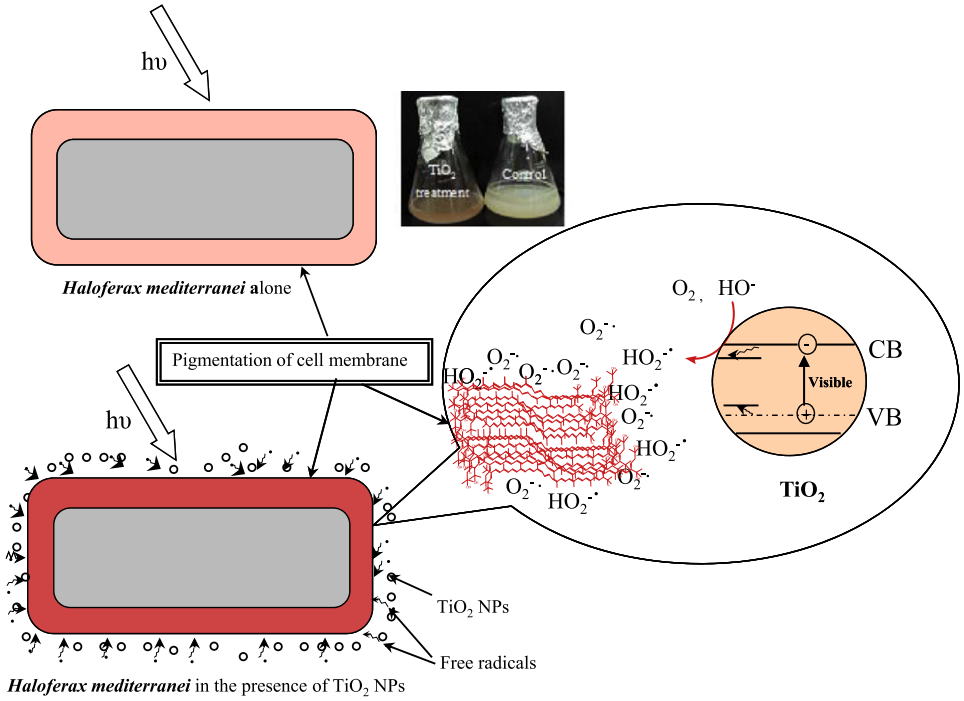


**Fig. 4.** Schematic representation speculating the possible $TiO_2$ NPs assisted enhanced biosynthesis of carotenoid pigments in *H. mediterranei* in response to the free radicals generated by $TiO_2$ NPs.

TLC and MALDI-MS analysis. The other peaks appeared from the TLC spots upon MALDI-MS analysis are believed to have resulted from fractionation of the carotenoid pigment.

### 3.4. Pt-ODT NP-LLME coupled with MALDI-MS for pigment detection from the halobacteria

Fig. 6A shows the procedures of a novel approach for extraction and preconcentration of the pigments from *H. mediterannei* by Pt-ODT NP-LLME coupled with the MALDI-MS detection. We have directly analyzed the pigments with three different concentrations such as 5, 2.5 and 1 μg. We were able to obtain detectable signals from the MALDI MS spectrum for 5 μg carotenoid concentration and the lower pigment concentrations (2.5 and 1 μg) failed to exhibit a decent spectrum (Fig. S4). Therefore from the crude pigment extract, 5 μg was diluted to 1 mL with deionized water. The carotenoid pigments were concentrated from the diluted extract using NP-LLME with 100 μL toluene containing different concentrations of Pt-ODT NPs. Fig. 6B shows the MALDI-MS spectra of molecules from the crude acetone extract of *H. mediterranei* concentrated via the Pt-ODT NPs prepared in toluene. From the diluted pigment solution, initially the LLME was carried out using toluene without Pt NPs but no successful pigment peaks were detected by MALDI-MS (Fig. 6B(a)). The addition of Pt-ODT NPs prepared in toluene for NP-LLME yielded mass spectral peaks which increased the number of pigment peaks as the nanoparticle concentration was increased in the toluene layer (Fig. 6B(b)–(c). In addition, the Pt-ODT NP-LLME also promoted the intensity of the pigment peaks with many times of enhancement (Fig. 6B(b)–(c)) which is an obvious evidence to prove the role of nanoparticle in LLME and MALDI-MS analysis, since the nanoparticles were already proven to be efficient matrices for versatile molecules [14]. After LLME of the diluted pigment extract with Pt-ODT NPs, the attachment of pigments on Pt ODT NPs were verified by FTIR analysis. The peak shifts in the PT ODT NPs after LLME confirm the attachment of pigment molecules on the surfaces of the Pt ODT NPs (Fig. S6). Since the interaction is electrostatic, those interactions have no influence during MALDI MS analysis. It proves that platinum nanoparticles functionalized with ODT interacts with molecules having acyclic structure of isoprenoid chain and thereby concentrates them on the nanoparticle surfaces.

As far as the carotenoid pigment is concerned, toluene extraction alone had never shown any carotenoid pigment peaks from the MALDI-MS analysis. However, a bacterioruberin peak at *m/z* 690 was observed in all the Pt-ODT NP-LLME approach, which was identified as trianhydrobacterioruberin based on the theoretical *m/z* prediction. The other bacterioruberin pigments such as monoanhydrobacterioruberin (*m/z* 723.427) and bacterioruberin (*m/z* 740.683) indicated by the symbol asterisk in Fig. 6B were extracted with Pt-ODT NPs at concentrations of 80 and 100 μg by NP-LLME and these pigments were not detected with 20, 40 and 60 μg Pt NPs in toluene. The peak (*m/z* 740.683) reproducibility during the MALDI MS detection is shown in Fig. S4. 2-isopentenyl-3,4-dehydrorhodopin, a carotenoid molecule reported previously can also be concentrated by Pt-ODT NP-LLME which was detected at *m/z* 620.440 from 40–100 μg. Therefore, this technique is very effective in halobacterial caroteinod detection. This Pt-ODT NP-LLME can also concentrate the other molecules which has isoprenyl chains, since the ODT functionalization is believed to attract the other lipid molecules having isoprenyl chains. The Pt-ODT NP-LLME also concentrated the other molecules that have isoprenyl chains which has been effectively proven by phosphatidyl glycerol phosphate at *m/z* 885.35 and a strong peak around 932 *m/z* (931.38 at 20 μg Pt-ODT NPs) which is believed to be a phosphatidyl glycerol phosphate (PGP) containing the molecule pyranose sugar [11]. A peak appeared at *m/z* 900.12 which can be assigned as the methylated PGP (theoretical *m/z* 899). (Fig. 6B(d)–(f)) indicated by the symbol •). The inset Figs. at Fig. 6B(d)–(f) show the magnified view of the peak at *m/z* 900.12.

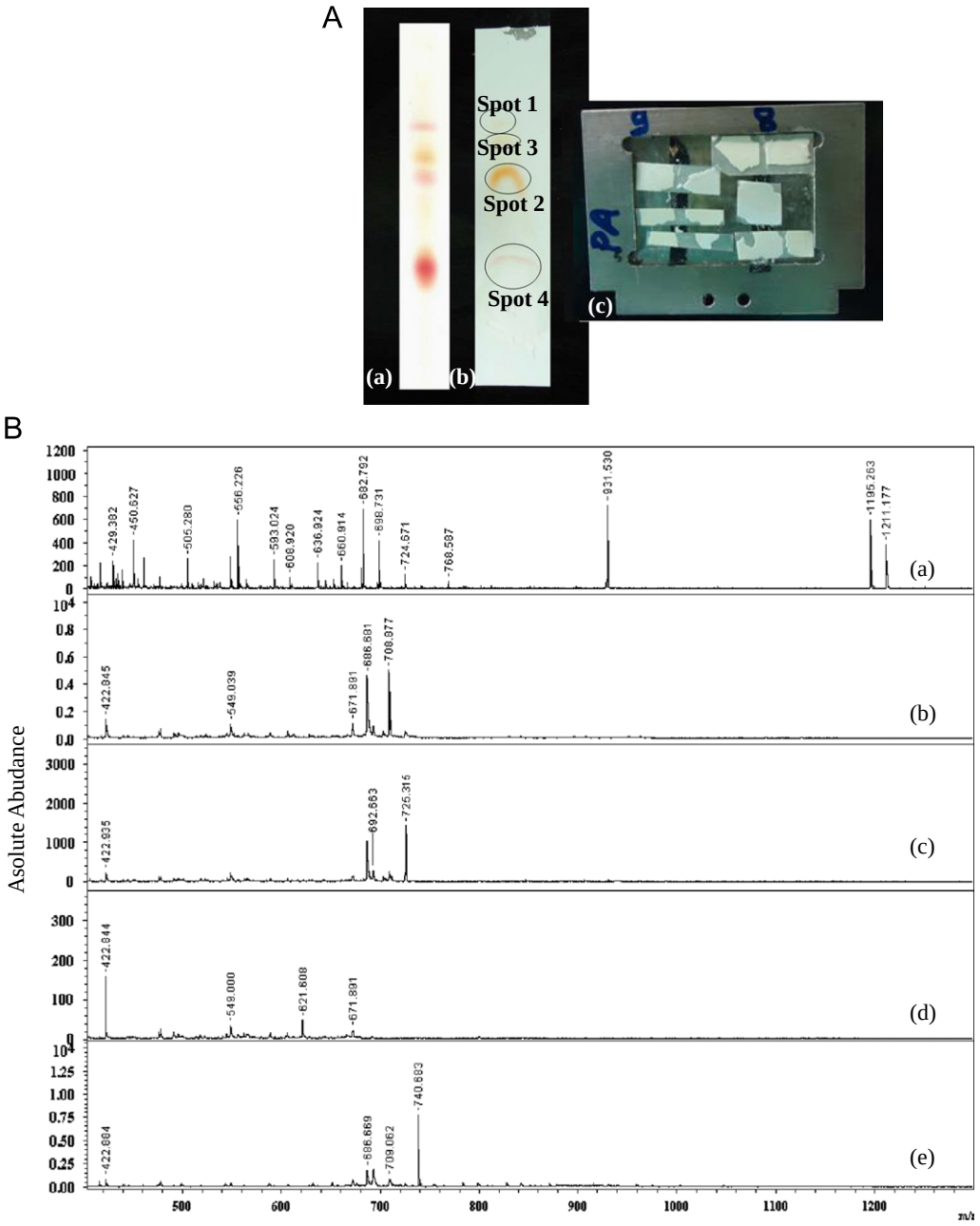


**Fig. 5.** (A) Photograph showing of the crude extract on the TLC plate for direct MALDI-MS analysis (a) TLC plate showing spots obtained after of crude extract; (b) Spots after addition of CHCA matrix; (c) Spots cut and loaded onto target plate. (B) Direct TLC MALDI-MS analysis of pigments after separation with acetone:*n*-heptane (1:1) and from crude extract. (a) MALDI-MS spectrum of crude acetone extract prior to TLC separation; (b) MALDI-MS spectrum of TLC spot 1; (c) MALDI-MS spectrum of TLC spot 2; (d) MALDI-MS spectrum of TLC spot 3; (e) MALDI-MS of TLC spot 4 (For interpretation of the references to color in this figure, the reader is referred to the web version of this article.).

As can be observed from Supplementary Fig. S5, through direct MALDI MS, it is possible to obtain carotenoid peaks at 5 and 2.5 μg concentrations, however no peaks were detected for 1 μg pigment concentration. In contrast, by employing Pt NPs based LLME approach, we were able to obtain carotenoid spectra even for 5 μg/mL concentration indicating that this technique is able to concentrate the pigment molecules from highly low concentration to a detectable level for MALDI MS.

Furthermore, it was reported that the enhancement of pigment production was optimized by varying the nutrients by a two-step approach [12]. But this is the first report where we use NPs to enhance pigment production. We have also used direct TLC MALDI MS for detecting the pigments enhanced using the NPs. Finally, we have used Pt ODT NPs assisted LLME for the concentration of extremely low quantity of pigments from the bacterial cell extracts and report their subsequent detection using MALDI MS.

## 4. Conclusion

We have used two NPs to demonstrate nanoparticle based pigment enhancement. Amidst the two NPs used, $TiO_2$ NPs appeared to be possess a more profound influence on enhancing the production of carotenoids by *H. mediterranei*. The NPs concentrations for maximizing pigment production were also optimized. Using, direct TLC-MALDI-MS, we enabled the rapid and sensitive detection of the nanoparticle-enhanced pigments. Besides, using Pt-ODT NP-LLME coupled with MALDI-MS, rapid

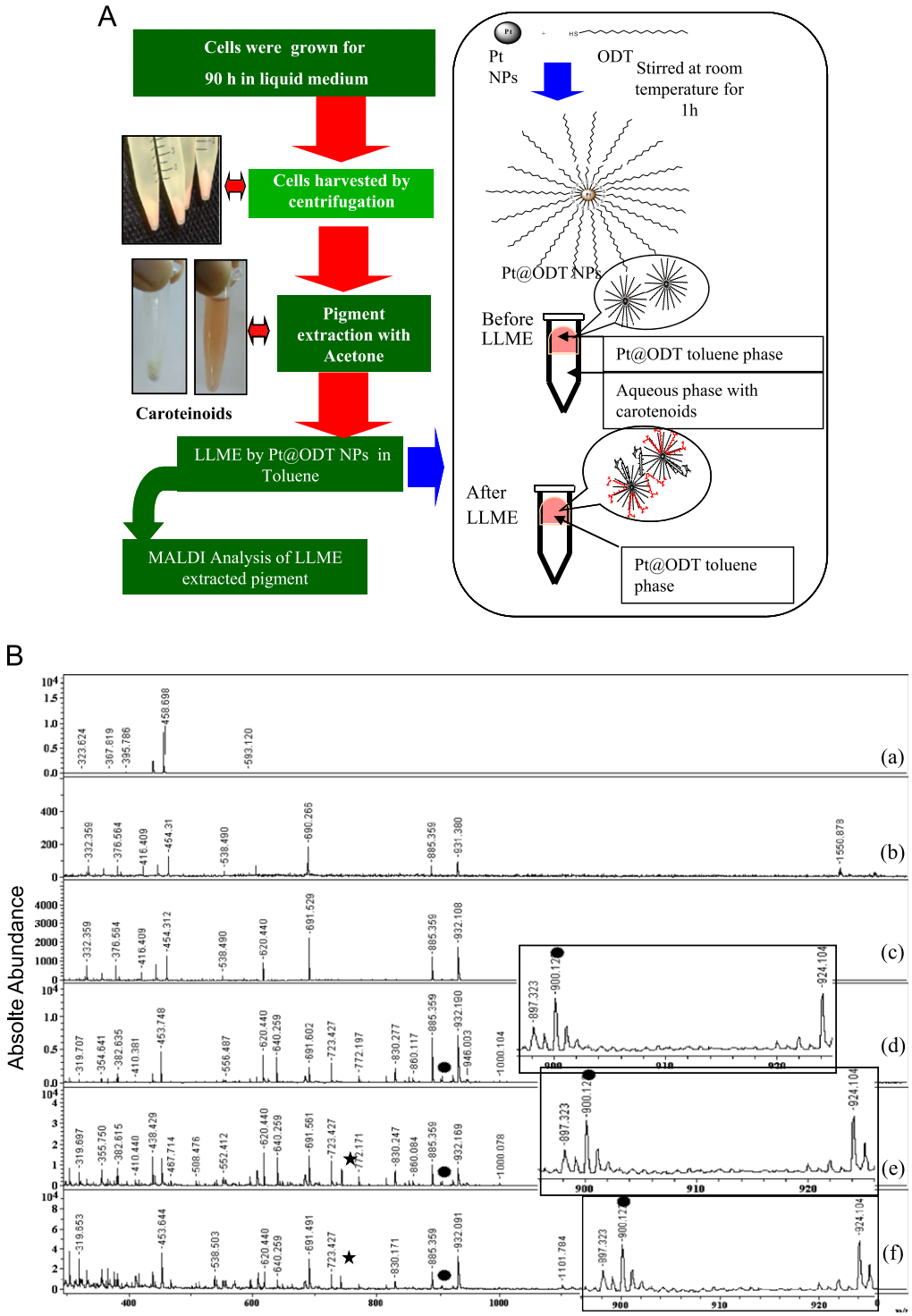


**Fig. 6.** (A) Schematic representation showing the steps involved in the concentration of pigments using Pt NPs functionalized with ODT in toluene by NP-LLME technique. (B) MALDI-MS analysis of pigments extracted from aqueous solution using Pt NPs functionalized with ODT in toluene by NP-LLME technique (a) MALDI-MS spectrum of toluene extract (without Pt-ODT NPs); (b) MALDI-MS spectrum of LLME with 100 μL toluene containing 20 μg Pt Nanoparticle functionalized with ODT; (c) MALDI-MS spectrum of LLME with 100 μL toluene containing 40 μg Pt nanoparticle functionalized with ODT; (d) MALDI-MS spectrum of LLME with 100 μL toluene containing 60 μg Pt nanoparticle functionalized with ODT; (e) MALDI-MS spectrum of LLME with 100 μL toluene containing 80 μg Pt nanoparticle functionalized with ODT; (f) MALDI-MS spectrum of LLME with 100 μL toluene containing 100 μg Pt nanoparticle functionalized with ODT. The bacterioruberin pigment at *m*/*z* 740.683 is represented by the symbol * and the other phospolipid peak at *m*/*z* 900.023 is marked with the symbol •.

and sensitive pigment detection from halobacteria could be demonstrated. We believe that the two novel approaches introduced from this study show the multi-faceted application of $TiO_2$ and Pt-ODT NPs in pigment detection from halobacteria and appear promising for sensitive detection of biomolecules of bacterial origin detection.

## Novelty statement

For the first time we use $TiO_2$ NPs for enhancing carotenoid production of *Haloferax mediterraneii* for the detection of the carotenoid pigments by direct TLC MALDI MS. We also report Pt

NP based microextraction of carotenoid pigments for MALDI MS detection.

## Appendix A. Supporting information

Supplementary data associated with this article can be found in the online version at http://dx.doi.org/10.1016/j.talanta.2013.01.005.

## References

[1] G. Schmid, Nanoparticles: From Theory to Application Edited by Günter Schmid, Wiley-VCH, 2004, pp. 611.
[2] O.V. Salata, J. Nanobiotechnol. 2 (2004) 1–6.
[3] M. Sharon, A.K. Choudhary, A. Kumar, J. Phytol. 2 (2010) 83–92.
[4] T.W. Goodwin, in: T.W. Goodwin (Ed.), The Biochemistry of Carotenoid, 1, Chapman and Hall Ltd., London, 1980, p. 290.
[5] M. Rønnekleiv, S. Rliaaen-Jensen, Biochem. Syst. Ecol. 23 (1995) 627–734.
[6] S.C. Kushwaha, M.B. Gochnauer, D.J. Kushner, M. Kates, Can. J. Microbiol. 20 (1974) 241–245.
[7] T. Saito, Y. Miyabe, H. Ide, O. Yamamoto, Radiat. Phys. Chem. 50 (1997) 267–269.
[8] D.J. Kushner, Microbial Life in Extreme Environments, Academic Press, London, 1978, pp. 318–368.
[9] H.R. Shahmohammadi, E. Asgarani, H. Terato, T. Saito, Y. Ohyama, K. Gekko, O. Yamamoto, H. Ide, J. Radiat. Res. (Tokyo) 39 (1998) 251–262.
[10] A. Ventosa, J.J. Nieto, World J. Microbiol. Biotechnol. 11 (1995) 85–94.
[11] S.M. Rivera, R. Canela-Garayoa., J. Chromatogr. A 1224 (2012) 1–10.
[12] C.J. Fang, K.L. Ku, M.H. Lee, N.W. Su, Bioresour. Technol. 101 (2010) 6487–6493.
[13] M.C. Fitzgerald, G.R. Parr, L.M. Smith., Anal. Chem. 65 (1993) 3204–3211.
[14] R.L. Vermillion-Salsbury, D.M. Hercules, Commun. Mass Spectrom. 16 (2002) 1575–1581.
[15] Y.T. Ke, S. Kailasa, H.-F. Wu, Z.-Y. Chen, Talanta 83 (2010) 178–184.
[16] K. Shrivas, H.F. Wu, Anal. Chem. 80 (2008) 2583–2589.
[17] D. Ai, X. Dai, Q. Li, C. Deng, S. Kang, China Particul. 2 (2004) 157–159.
[18] S. Qourzal, M. Tamimi, A. Assabbane, A. Bouamrane, A. Nounah, L. Laanab, Y. Ait lchou, J. Appl. Sci. (2006) 1539–1553.
[19] S. Chen, K.J. Kimura, Phys. Chem. B 105 (2001) 5397–5403.
[20] M. Manikandan, L. Pasic, V. Kannan, Bioresour. Technol. 100 (2009) 3107–3112.
[21] S. Liaaen-Jensen, A. Jensen, Methods Enzymol. 23 (1971) 586–602.
[22] I. Fenoglio, G. Greco, S. Livraghi, B. Fubini, Chem. Eur. J. 15 (2009) 4614–4621.